Functionalization of Indium Tin Oxide

Victor M. Bermudez,*,† Alan D. Berry,‡ Heungsoo Kim,§ and Alberto Piqué§

Electronics Science and Technology Division, Chemistry Division, and Material Science and Technology Division, Naval Research Laboratory, 4555 Overlook Avenue, S.W., Washington, DC 20375-5320

Received June 1, 2006. In Final Form: September 20, 2006

The preparation and functionalization of ITO surfaces has been studied using primarily X-ray photoemission spectroscopy and infrared reflection−absorption spectroscopy (IRRAS) and the reagents *n*-hexylamine and *n*-octyltrimethoxysilane (OTMS). Particular attention has been paid to characterization of the surfaces both before and after functionalization. Surfaces cleaned by ultraviolet (UV)/ozone treatment and subsequently exposed to room air have ∼0.5−0.8 monolayers (ML) of adsorbed impurity C. Most is in the form of aliphatic species, but as much as one-half is partially oxidized and consists of C−OH, C−O−C, and/or >C═O groups. The coverage of these species can be reduced by cleaning in organic solvents prior to UV/ozone treatment. The OH coverage on the ITO surfaces studied here is relatively small (∼1.0 OH nm^{-2}), based on the Si coverage after reaction with OTMS. A satellite feature in the O 1s XPS spectrum, often suggested to be a quantitative measure of adsorbed OH, receives a significant contribution from sources not directly related to hydroxylated ITO. *n*-Hexylamine adsorbs, at a saturation coverage of ∼0.08 ML, via a Lewis acid−base interaction. The particular acid site has not been conclusively identified, but it is speculated that surface Sn sites may be involved. For OTMS, a saturation coverage of about 0.21 ML is found, and the C/Si atom ratios suggest that some displacement of preadsorbed organic impurities occurs during adsorption. The alkyl chain of adsorbed OTMS is disordered, with no preferred stereoisomer. However, the chain appears to lie mainly parallel to the surface with the plane defined by the terminal $CH_3-CH_2-CH_2-$ segment oriented essentially perpendicular to the surface.

1. Introduction

The functionalization of (attachment of organic ligands to) the surface of indium−tin−oxide (ITO) has been the subject of intense interest due to the potential applications in fabricating transparent contacts for organic optoelectronic devices and in sensors for chemical and/or biological reagents. Nevertheless, the structure of the functionalized surface and the nature of the chemical bonding at the molecule/ITO interface remain, in general, poorly understood. The particular application that motivated the present investigation is an interest in using bifunctional coupling agents in a wet-chemical procedure to tether quantum dots to an ITO surface. For this purpose, it is necessary to establish the chemical and geometrical structure of the organic adlayer.

Some work[1−3] in this area has been done largely or entirely in ultrahigh vacuum (UHV). However, the vast majority of ITO functionalization studies have been performed wet-chemically using a wide variety of reagents including organic and organometallic alkoxysilanes,[2−12] amines,[13−16] carboxylic acids,[1,17−23] organic and inorganic halides,[24−29] phosphonic acids,[30−33] and thiols[1,22,34,35] as well as bifunctional molecules.[2,6,8,13,14] The

* To whom correspondence should be addressed. E-mail: victor.bermudez@nrl.navy.mil.

† Electronics Science and Technology Division, Code 6876.

‡ Chemistry Division, Code 6123.

§ Material Science and Technology Division, Code 6364.

(1) Yan, C.; Zharnikov, M.; Gölzhäuser, A.; Grunze, M. *Langmuir* **2000**, *16*, 6208.

(2) Purvis, K. L.; Lu, G.; Schwartz, J.; Bernasek, S. L. *J. Am. Chem. Soc.* **2000**, *122*, 1808. Span, A. R.; Bruner, E. L.; Bernasek, S. L.; Schwartz, J. *Langmuir* **2001**, *17*, 948

(3) Schwartz, J.; Gawalt, E. S.; Lu, G.; Milliron, D. J.; Purvis, K. L.; Woodson, S. J.; Bernasek, S. L.; Bocarsly, A. B.; VanderKam, S. K. *Polyhedron* **2000**, *19*, 505. Schwartz, J.; Bruner, E. L.; Koch, N.; Span, A. R.; Bernasek, S. L.; Kahn, A. *Synth. Met.* **2003**, *138*, 223.

(4) Nishiyama, K.; Ishida, H.; Taniguchi, I. *J. Electroanal. Chem.* **1994**, *373*, 255.

(5) Ho, P. K. H.; Granström, M.; Friend, R. H.; Greenham, N. C. *Adv. Mater.* **1998**, *10*, 769.

(6) VanderKam, S. K.; Gawalt, E. S.; Schwartz, J.; Bocarsly, A. B. *Langmuir* **1999**, *15*, 6598.

(7) Yamada, H.; Imahori, H.; Nishimura, Y.; Yamazaki, I.; Fukuzumi, S. *Chem. Commun.* **2000**, 1921.

(8) Sfez, R.; De-Zhong, L.; Turyan, I.; Mandler, D.; Yitzchaik, S. *Langmuir* **2001**, *17*, 2556.

(9) Hillebrandt, H.; Tanaka, M. *J. Phys. Chem. B* **2001**, *105*, 4270.

(10) Markovich, I.; Mandler, D. *J. Electroanal. Chem.* **2001**, *500*, 453.

(11) Lee, J.; Jung, B.-J.; Lee, J.-I.; Chu, H. Y.; Do, L.-M.; Shim, H.-K. *J. Mater. Chem.* **2002**, *12*, 3494.

(12) Sigaud, P.; Chazalviel, J.-N.; Ozanam, F.; Lahlil, K. *Appl. Surf. Sci.* **2003**, *218*, 54.

(13) Oh, S.-Y.; Yun, Y.-J.; Hyung, K.-H.; Han, S.-H. *New J. Chem.* **2004**, *28*, 495. Oh, S.-Y.; Yun, Y.-J.; Kim, D.-Y.; Han, S.-H. *Langmuir* **1999**, *15*, 4690.

(14) Kim, C. O.; Hong, S.-Y.; Kim, M.; Park, S.-M.; Park, J. W. *J. Colloid Interface Sci.* **2004**, *277*, 499.

(15) Hyung, K.-H.; Han, S.-H. *Synth. Met.* **2003**, *137*, 1441.

(16) Zotti, G.; Schiavon, G.; Zecchin, S.; Berlin, A.; Pagani, G.; Canavesi, A. *Langmuir* **1997**, *13*, 2694.

(17) Meyer, T. J.; Meyer, G. J.; Pfennig, B. W.; Schoonover, J. R.; Timpson, C. J.; Wall, J. F.; Kobusch, C.; Chen, X.; Peek, B. M.; Wall, C. G.; Ou, W.; Erickson, B. W.; Bignozzi, C. A. *Inorg. Chem.* **1994**, *33*, 3952.

(18) Tanaka, T.; Honda, Y.; Tani, T.; Terahara, A.; Tabe, Y.; Sugi, M. *Jpn. J. Appl. Phys.* **1994**, *33*, 295. Tanaka, T.; Honda, Y.; Sugi, M. *Jpn. J. Appl. Phys.* **1995**, *34*, 3250.

(19) Napier, M. E.; Thorp, H. H. *Langmuir* **1997**, *13*, 6342.

(20) Carrara, M.; Nüesch, F.; Zuppiroli, L. *Synth. Met.* **2001**, *121*, 1633.

(21) Fang, A.; Ng, H.; Li, S. F. Y. *Langmuir* **2001**, *17*, 4360.

(22) Brewer, S. H.; Brown, D. A.; Franzen, S. *Langmuir* **2002**, *18*, 6857.

(23) Armstrong, N. R.; Carter, C.; Donley, C.; Simmonds, A.; Lee, P.; Brumbach, M.; Kippelen, B.; Domercq, B.; Yoo, S. *Thin Solid Films* **2003**, *445*, 342.

(24) Chen, K.; Herr, B. R.; Singewald, E. T.; Mirkin, C. A. *Langmuir* **1992**, *8*, 2585.

(25) Malinsky, J. E.; Jabbour, G. E.; Shaheen, S. E.; Anderson, J. D.; Richter, A. G.; Marks, T. J.; Armstrong, N. R.; Kippelen, B.; Dutta, P.; Peyghambarian, N. *Adv. Mater.* **1999**, *11*, 227. Malinsky, J. E.; Veinot, J. G. C.; Jabbour, G. E.; Shaheen, S. E.; Anderson, J. D.; Lee, P.; Richter, A. G.; Burin, A. L.; Ratner, M. A.; Marks, T. J.; Armstrong, N. R.; Kippelen, B.; Dutta, P.; Peyghambarian, N. *Chem. Mater.* **2002**, *14*, 3054.

(26) Cui, J.; Huang, Q.; Wang, Q.; Marks, T. J. *Langmuir* **2001**, *17*, 2051.

(27) Ganzorig, C.; Kwak, K.-J.; Yagi, K.; Fujihira, M. *Appl. Phys. Lett.* **2001**, *79*, 272.

(28) Harrison, K. E.; Kang, J. F.; Haasch, R. T.; Kilbey, S. M., II. *Langmuir* **2001**, *17*, 6560.

(29) Luscombe, C. K.; Li, H.-W.; Huck, W. T. S.; Holmes, A. B. *Langmuir* **2003**, *19*, 5273.

10.1021/la061578a
Published on Web 11/07/2006

Report Documentation Page

Form Approved
OMB No. 0704-0188

1. REPORT DATE	2. REPORT TYPE	3. DATES COVERED
SEP 2006		**00-00-2006 to 00-00-2006**

4. TITLE AND SUBTITLE	5a. CONTRACT NUMBER
Functionalization of Indium Tin Oxide	5b. GRANT NUMBER
	5c. PROGRAM ELEMENT NUMBER
6. AUTHOR(S)	5d. PROJECT NUMBER
	5e. TASK NUMBER
	5f. WORK UNIT NUMBER
7. PERFORMING ORGANIZATION NAME(S) AND ADDRESS(ES) **Naval Research Laboratory,Electronics Science and Technology DiVision,4555 Overlook Avenue SW,Washington,DC,20375**	8. PERFORMING ORGANIZATION REPORT NUMBER
9. SPONSORING/MONITORING AGENCY NAME(S) AND ADDRESS(ES)	10. SPONSOR/MONITOR'S ACRONYM(S)
	11. SPONSOR/MONITOR'S REPORT NUMBER(S)

12. DISTRIBUTION/AVAILABILITY STATEMENT
Approved for public release; distribution unlimited

13. SUPPLEMENTARY NOTES

14. ABSTRACT

15. SUBJECT TERMS

16. SECURITY CLASSIFICATION OF:			17. LIMITATION OF ABSTRACT	18. NUMBER OF PAGES	19a. NAME OF RESPONSIBLE PERSON
a. REPORT	b. ABSTRACT	c. THIS PAGE			
unclassified	**unclassified**	**unclassified**	**Same as Report (SAR)**	**13**	

bifunctional reagents permit, in principle, subsequent reactions in which the free end is used to anchor another chemical species. In some cases, the adsorbate is implicitly assumed to form a densely packed self-assembled monolayer (SAM) with few if any data provided specifically to characterize the actual structure. One exception is the work of Yan et al.[1] in which ITO was cleaned by Ar^+ bombardment in a UHV system and then exposed to alkanethiols or to carboxylic acids either in situ or in a liquid medium. The functionalized surfaces were then studied using the H_2O contact angle (CA) and the C 1s near-edge X-ray absorption fine structure (NEXAFS) spectrum, which established the formation of SAMs. In this case, Ar^+ bombardment may be required to form a high density of reactive (i.e., damaged) surface sites, which in turn leads to a densely packed organic layer.

The issue of functionalization is closely coupled to the question of ITO surface chemistry. This subject remains controversial, particularly regarding the presence or absence of surface OH groups and their role in the attachment chemistry. In some UHV studies,[2,3] the substrate preparation procedure was specifically designed to yield a high OH coverage, which was detectable via X-ray photoelectron spectroscopy (XPS) and infrared (IR) spectroscopy and which was demonstrably involved in the functionalization reaction. On the other hand, for "practical" ITO surfaces (those not prepared and maintained in an atomically clean state in UHV), the surface OH content, its dependence on cleaning procedure, and its correlation with reactivity are uncertain.[36,37] Nevertheless, most ITO functionalization studies assume a high coverage of OH as the chemically active sites, often without characterization. In some cases, the presence of surface OH is deduced from the appearance of a particular component in the O 1s XPS (see below); however, the exact interpretation of this feature is somewhat uncertain.

Practical ITO surfaces also exhibit, in XPS, an adventitious carbon contamination, which is an unavoidable consequence of exposure to room air. There is, in fact, evidence[37,38] that clean ITO surfaces in UHV can readily adsorb small amounts of hydrocarbon impurities (if present) from the background. The C impurity on practical surfaces, typically at a level described as an "atomic fraction of ∼10%", is generally ignored in ITO functionalization studies. The C impurity is confined to the surface, as shown[2,37] by its easy removal with only light Ar-ion bombardment. Hence, the "atomic fraction" description is inappropriate, except as a measure of the relative C coverage, because it implies a model in which the C is uniformly distributed throughout the XPS sampling depth (∼19 Å under the present conditions, see Supporting Information). When the amount of surface C is expressed, more appropriately, as a fraction of a monolayer, it is found that an "atomic fraction of 10%" corresponds to about 0.8 monolayers (MLs) where 1 ML is defined here as one C atom per ITO surface site. The impurity is presumably in the form of organic molecular species, with an unknown number of C atoms per molecule. Hence, the coverage in terms of molecules per cm^2 is smaller than the number of C atoms per cm^2. Nevertheless, a substantial fraction of the surface is covered by C, which can block the functionalization reaction unless it is displaced by the reagent or by whatever solvent might be employed in the reaction. In many cases, the surface C is partially oxidized, and the resulting functional groups (e.g., C−OH) could also act as reactive sites, as suggested previously.[37] A more complete discussion of OH and C on practical ITO surfaces is given below.

In the present work, we apply primarily XPS and infrared reflection−absorption spectroscopy (IRRAS) to a determination of the structure and bonding of the functionalized surface layer. Because the adsorbates of interest all involve hydrophobic *n*-alkyl chains, measurements of the CA will also be used in an independent assessment of the extent of adsorbate coverage. Particular attention is paid to the chemical characterization of the ITO surface both before and after functionalization. Three reagents are employed in this study: (1) an "inert" hydrocarbon, *n*-hexane, as a "baseline" reagent; (2) a primary amine, *n*-hexylamine [$CH_3(CH_2)_4CH_2{-}NH_2$], for probing Lewis acid sites; and (3) a substituted silane, *n*-octyltrimethoxysilane [OTMS, $CH_3(CH_2)_6CH_2{-}Si(OCH_3)_3$], for probing surface OH sites.

2. Experimental Details

2.1. Reagents and Chemicals. Xylene and methanol (certified ACS reagents), hexane (HPLC grade), and acetone (National Formulary/National Food Chemicals Codex/European Pharmocopia grade) were purchased from Fisher Scientific. Triply distilled H_2O was obtained from a quartz still. *n*-Hexylamine (>99.5%) was purchased from Fluka and vacuum distilled according to RT ∼ 0 °C ∼ −78 °C ∼ −196 °C under a dynamic vacuum. The −78 °C fraction was collected and stored in vacuo over activated 3A molecular sieves. The OTMS was purchased from Gelest, Inc., and vacuum distilled according to RT ∼ 0 °C ∼ −196 °C under a dynamic vacuum. The 0 °C fraction was collected and stored under vacuum. Nuclear magnetic resonance (NMR) and IR spectra of the purified reagents are given in the Supporting Information.

2.2. Substrate Growth and Preparation. The XPS and CA measurements were done primarily on films of ITO on Corning 1737 glass purchased as 36 × 36 × 0.11 cm^3 sheets from Colorado Concept Coatings, Longmont, CO. Henceforth, this material will be referred to as "commercial ITO". Samples were cut from the inner 18 × 18 cm^2 section of the sheet. The maximum ITO sheet resistance was listed as 9−15 Ω/□ and the coating thickness as 120−160 nm.

The IRRAS experiments were performed on thin films of ITO deposited on an Au mirror by pulsed-laser deposition[39,40] (PLD). The reason for the use of an Au substrate is discussed below. A thin Cr film was first vapor-deposited on a fused-silica slide to serve as an adhesion layer, followed by deposition of a 500 nm-thick Au film. The bare silica, prior to metal deposition, was subjected to a series of cleaning steps (described below), and the same process was applied after Au deposition. These treatments were necessary to ensure uniformity of the Au and ITO films. A 30−50 nm-thick layer of ITO was then grown on the clean Au mirror using a KrF excimer laser (Lambda Physics LPX 305, $\lambda = 248$ nm, 30 ns pulse duration).

(30) Appleyard, S. F. J.; Day, S. R.; Pickford, R. D.; Willis, M. R. *J. Mater. Chem.* **2000**, *10*, 169.
(31) Besbes, S.; Ltaief, A.; Reybier, K.; Ponsonnet, L.; Jaffrezic, N.; Davenas, J.; Ben Ouada, H. *Synth. Met.* **2003**, *138*, 197.
(32) Hanson, E. L.; Guo, J.; Koch, N.; Schwartz, J.; Bernasek, S. L. *J. Am. Chem. Soc.* **2005**, *127*, 10058.
(33) Koh, S. E.; McDonald, K. D.; Holt, D. H.; Dulcey, C. S.; Chaney, J. A.; Pehrsson, P. E. *Langmuir* **2006**, *22*, 6249.
(34) Gardner, T. J.; Frisbie, C. D.; Wrighton, M. S. *J. Am. Chem. Soc.* **1995**, *117*, 6927.
(35) Kondo, T.; Takechi, M.; Sato, Y.; Uosaki, K. *J. Electroanal. Chem.* **1995**, *381*, 203.
(36) Donley, C.; Dunphy, D.; Paine, D.; Carter, C.; Nebesny, K.; Lee, P.; Alloway, D.; Armstrong, N. R. *Langmuir* **2002**, *18*, 450. Donley, C. L.; Dunphy, D.; Zangmeister, R. A. P.; Nebesny, K. W.; Armstrong, N. R. In *Conjugated Polymer and Molecular Interfaces*; Salaneck, W. R., Seki, K., Kahn, A., Pireaux, J.-J., Eds.; Marcel Dekker: New York, 2002; p 269.
(37) Chaney, J. A.; Pehrsson, P. E. *Appl. Surf. Sci.* **2001**, *180*, 214. Chaney, J. A.; Koh, S. E.; Dulcey, C. S.; Pehrsson, P. E. *Appl. Surf. Sci.* **2003**, *218*, 258.
(38) Tadayyon, S. M.; Griffiths, K.; Norton, P. R.; Tripp, C.; Popovic, Z. *J. Vac. Sci. Technol., A* **1999**, *17*, 1773.
(39) Kim, H.; Piqué, A.; Horwitz, J. S.; Mattoussi, H.; Murata, H.; Kafafi, Z. H.; Chrisey, D. B. *Appl. Phys. Lett.* **1999**, *74*, 3444. Kim, H.; Horwitz, J. S.; Piqué, A.; Gilmore, C. M.; Chrisey, D. B. *Appl. Phys. A: Mater. Sci. Process.* **1999**, *69*, S447.
(40) Kim, H.; Horwitz, J. S.; Kushto, G.; Piqué, A.; Kafafi, Z. H.; Gilmore, C. M.; Chrisey, D. B. *J. Appl. Phys.* **2000**, *88*, 6021. Kim, H.; Gilmore, C. M.; Piqué, A.; Horwitz, J. S.; Mattoussi, H.; Murata, H.; Kafafi, Z. H.; Chrisey, D. B. *J. Appl. Phys.* **1999**, *86*, 6451.

The properties of the PLD films are described in refs 39 and 40, and further details concerning the PLD growth are given in the Supporting Information.

Prior to functionalization, the ITO (either commercial or PLD) was subjected to solvent and ultraviolet (UV)/ozone cleaning. Solvent cleaning consisted of the following steps: (a) rinsing with xylene, boiling in xylene (10 min), rinsing with xylene, (b) rinsing with acetone, boiling in acetone (10 min), rinsing with acetone, (c) rinsing with methanol, boiling in methanol (10 min), rinsing in methanol, and (d) rinsing with triply distilled H_2O, boiling in triply distilled H_2O (10 min).

This was followed by cleaning at 140 °C for 20 min using a Samco International (Kyoto, Japan) model UV-1 UV-ozone stripper/cleaner, boiling in triply distilled H_2O (10 min), and drying under N_2 gas. The purpose of the second boiling-H_2O treatment was to maximize the surface OH content as much as possible and to passivate any surface sites that might react with airborne CO_2 or hydrocarbons during subsequent handling and processing in room air. Dry samples were transferred immediately to clean Pyrex vacuum containers and evacuated with a liquid-N_2-cooled zeolite sorption pump and a liquid-N_2-trapped oil diffusion pump to a base pressure $\leq 1 \times 10^{-6}$ Torr. After evacuation, the containers were backfilled with liquid-N_2 boil-off gas and evacuated. The backfilling/evacuation cycle was done a total of three times. Untreated samples were then backfilled a fourth time and closed.

2.3. Characterization Methods. X-ray photoemission spectroscopy was carried out in UHV ($\sim 1 \times 10^{-9}$ Torr) using a hemispherical analyzer system with a monochromated Al Kα source. The combined resolution of the source and analyzer was about 0.33 eV. Photoelectron takeoff angles, with respect to the surface normal, were typically either $\theta = 0$ or 60°, the latter giving a 2-fold (1/cos(60°)) reduction in sampling depth (i.e., an increased surface sensitivity).

Least-squares fitting[41] of core-level spectra with a sum of Gaussians and a polynomial background function was done to determine peak areas and to separate overlapping features. Unless otherwise noted, pure Gaussian line shapes were used, with no Lorentzian component, and the intensity, position, and full-width at half-maximum (fwhm) of each component were unconstrained in the fitting process. The background coefficients were obtained as part of the fit, and no background subtraction or smoothing of any kind was done before fitting.[41] Further comments regarding the fitting procedure will be made in appropriate sections below. A detailed description of the procedures used to determine sample composition and adsorbate coverage from XPS peak areas is given in the Supporting Information. The binding energy (BE) scale was shifted to position the C 1s peak (due to aliphatic impurities incurred during exposure to room air) at 285.0 eV (ref 42).

The question of "beam damage" (i.e., molecular decomposition caused either by the X-ray beam or by secondary electrons) is a concern[1,43,44] in XPS of organic adsorbates. Beam damage is reduced in the present work by the use of a monochromatic X-ray source, but the effect is nevertheless noticeable as a slow, monotonic decrease in the apparent C coverage with prolonged X-ray irradiation. Hence, data used for the quantitative determination of C coverage were recorded early in the sequence of data sets. Damage in the form of a structural change without concurrent desorption of molecular fragments is more difficult to diagnose without a technique (such as ultraviolet photoemission spectroscopy) that is sensitive to chemical bonding.

The CA for triply distilled H_2O on the ITO film was measured under ambient conditions using a model VCA 2500XE video contact angle system from AST Products, Inc. (Billerica, MA). One microliter (μL) of H_2O was added to the film using a 100 μL syringe, and the contact angle was measured immediately. Contact angle values reported are averages of at least three measurements.

2.4. IR Spectroscopy. The IRRAS data were recorded using a Fourier transform spectrometer with (except where noted) a liquid-N_2-cooled "narrow-band" (MCT-A) $Hg_xCd_{1-x}Te$ detector and a variable-angle external-reflection accessory. Data were recorded at 8 cm^{-1} resolution with p-polarized radiation incident at an angle of nominally 82° with respect to the surface normal. Spectra recorded at 4 cm^{-1} resolution showed no additional structure. Typically, 2000 scans were averaged over about 20 min, and triangle apodization with 2-fold zero-filling was used in processing the interferogram. The sample was maintained in the dry-N_2 purge of the spectrometer during measurement. When necessary, a software correction was applied to remove weak residual absorption due to traces of atmospheric H_2O. The data are presented in the form of $(\delta R/R)_p$, the fractional change in the p-polarized reflectance of the bare ITO/Au substrate caused by the treatment of interest. Here, $(\delta R/R)_p \equiv (R_p^{exp} - R_p^{bare})/R_p^{bare}$, where R^{bare} and R^{exp} are the reflectances of the bare and exposed surfaces, respectively.

The Au substrate mentioned above functioned as a buried metal layer (BML) to enhance the external-reflection IRRAS sensitivity[45] to adsorbates relative to that attainable for bulk ITO. The IR optical properties of the BML structure are essentially those of the metal; hence, the so-called "metal surface selection rule[46]" is in effect. The only normal modes that can be detected are those with a finite projection of the dynamic dipole moment along the surface normal, and these are observable only in p-polarization and at a near-grazing angle of incidence. An ITO film with a sufficiently high free-electron density can exhibit "metal-like" optical properties in the mid-IR. For large adsorbate molecules (i.e., those with many $-CH_2-$ groups), the IRRAS sensitivity in this case is such that spectra with a good signal-to-noise ratio (SNR) in the C−H stretching range can sometimes be obtained[10,18,22,28] in a single external reflection for a thick ITO layer on glass. However, for the smaller molecules studied here, it was found that such a bulk ITO substrate did not provide adequate IRRAS data. The Supporting Information provides results of model calculations showing the enhanced IRRAS sensitivity for an organic layer on ITO with a BML.

2.5. Functionalization Procedure. Functionalization was done by exposure to the reagent vapor, rather than to a solution, to minimize contact with extraneous organic species including polymerized organosilanes. As noted above and elsewhere in this study, ITO surfaces have an affinity for such contaminants, which complicates studies of functionalization. The treatments were performed using the Pyrex vacuum system described above. Reagents were condensed at −196 °C into sidearms on the vacuum containers and allowed to warm to ambient temperature. For OTMS, the main tube containing the ITO substrate was warmed to 50−70 °C in a heating mantle during the procedure. At the conclusion of the treatment, the container was evacuated through liquid-N_2-cooled traps, followed by backfilling with N_2 gas and evacuation as described above.

3. Results and Discussion

3.1. Infrared Characterization of PLD ITO Films. Figure 1 shows IRRAS data for a typical ITO/Au sample, referenced to the reflectance spectrum of the bare Au substrate. Weak features near 1600 and 3600 cm^{-1} are due to a trace of atmospheric H_2O in the spectrometer, and a weak structure near 2900 cm^{-1} arises from a small amount of hydrocarbon contamination on the Au film.

The band at $\sim$6400 cm^{-1} ($\lambda = 1.56$ μm) results from free-carrier plasmon excitation, which has been discussed previously[40,47−51] for ITO films on glass, and indicates an electron

(41) Wertheim, G. K.; Dicenzo, S. B. *J. Electron Spectrosc. Relat. Phenom.* **1985**, *37*, 57.
(42) Briggs, D. *Surface Analysis of Polymers by XPS and Static SIMS*; Cambridge University Press: Cambridge, 1998.
(43) Zharnikov, M.; Grunze, M. *J. Vac. Sci. Technol., B* **2002**, *20*, 1793.
(44) Frydman, E.; Cohen, H.; Maoz, R.; Sagiv, J. *Langmuir* **1997**, *13*, 5089.
(45) Bermudez, V. M. *J. Vac. Sci. Technol., A* **1992**, *10*, 152.
(46) Chabal, Y. J. *Surf. Sci. Rep.* **1988**, *8*, 211.
(47) Brewer, S. H.; Franzen, S. *J. Phys. Chem. B* **2002**, *106*, 12986; *J. Alloys Compd.* **2002**, *338*, 73.
(48) Solieman, A.; Aegerter, M. A. *Thin Solid Films* **2006**, *502*, 205.
(49) Davenas, J.; Besbes, S.; Ben Ouada, H. *Synth. Met.* **2003**, *138*, 295.
(50) Brewer, S. H.; Franzen, S. *Chem. Phys.* **2004**, *300*, 285.
(51) Rhodes, C.; Franzen, S.; Maria, J.-P.; Losego, M.; Leonard, D. N.; Laughlin, B.; Duscher, G.; Weibel, S. *J. Appl. Phys.* **2006**, *100*, 054905.

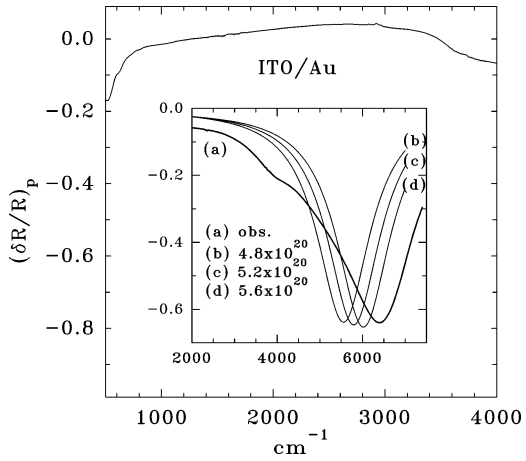

Figure 1. IRRAS data for a bare, UV/ozone-cleaned PLD ITO/Au sample obtained in p-polarization at an angle of incidence of $\theta = 82°$ and referenced to a bare Au substrate. An MCT-B "wide-band" detector was used. The inset shows (a) data recorded in the near-IR using an InSb detector together with (b−d) $(\delta R/R)_p$ computed at $\theta = 82°$ for an ITO film on Au. The ITO is modeled using a Drude function (see text) with $\epsilon_\infty = 3.8$, $m^* = 0.40m_e$, $\gamma = \hbar/\tau = 1 \times 10^3$ cm^{-1}, and electron densities of $n = 4.8$, 5.2, or 5.6×10^{20} cm^{-3}.

density of about 7.0×10^{20} cm^{-3} (see below). The optical effect of plasmon excitation in the ITO is qualitatively different for a BML structure versus an ITO film on a dielectric substrate. Figure 1 (inset) shows $(\delta R/R)_p$ calculated using the Fresnel relations for a thin ITO film on an Au substrate (see Supporting Information). The ITO is modeled using the Drude complex dielectric function:

$$\tilde{\epsilon}(\omega) = \epsilon_\infty - \omega_p{}^2/(\omega^2 + i\omega/\tau) \qquad (1)$$

where $\omega_p = (4\pi ne^2/m^*)^{1/2}$ is the plasmon frequency, ϵ_∞ is the high-frequency dielectric constant, and τ is the scattering lifetime. In ω_p, n is the carrier density, and e and m^* are the electron charge and effective mass. The model calculations used $\epsilon_\infty = 3.8$ (ref 47), $m^* = 0.40m_e$ (ref 50, where m_e is the electron mass), and values for n and $\gamma = \hbar/\tau$ sufficient to give a $(\delta R/R)_p$ spectrum that is similar to the experimental result. No attempt is made to fit the actual data, only to establish that the reflectance feature near 6400 cm^{-1} has been correctly identified and to show the high degree of sensitivity of the peak energy to n.

To make use of the plasmon resonance, it is necessary to obtain the relationship between ω_p and the frequency, ω_{min}, of the minimum in $(\delta R/R)_p$. For a dielectric film on a metallic substrate in the thin-film limit ($4\pi dn_f \cos\theta/\lambda \ll 1$, where n_f is the real index of refraction of the film), $(\delta R/R)_p$ measured in air is given by[46]

$$(\delta R/R)_p \approx (8\pi d/\lambda) \sin\theta \cdot \tan\theta \cdot \mathrm{Im}(-1/\tilde{\epsilon}_z) \qquad (2)$$

where d is the film thickness and $\tilde{\epsilon}_z$ is the surface-normal component of the complex dielectric function of the film. The angle of incidence, θ, is such that $\tan^2\theta < |\tilde{\epsilon}_m|$, where $\tilde{\epsilon}_m$ is the complex dielectric function of the metal and $|\tilde{\epsilon}_m| = n_m{}^2 + k_m{}^2$ in terms of the real and imaginary indices of refraction. For Au, eq 2 is valid at $\hbar\omega = 6000$ cm^{-1} for $\theta < 85°$. With $(\hbar\omega)^2 \gg \gamma^2$, which applies in the present case, and the assumption that the film $\tilde{\epsilon}$ is isotropic, substituting eq 1 into eq 2 gives $\omega_{min} = \omega_p/\sqrt{\epsilon_\infty}$. With $n = 7.0 \times 10^{20}$ cm^{-3}, one obtains $\hbar\omega_p = 1.252 \times 10^4$ cm^{-1} and $\hbar\omega_{min} = 6424$ cm^{-1}, consistent with the experimental and numerical results shown in Figure 1 (inset). The n value thus obtained is only approximate because ω_p depends on the ratio n/m^*, and the exact m^* is uncertain.

The magnitude of the plasmon feature in $(\delta R/R)_p$ is a factor of $\sim 10^2$ greater than that of the adsorbate-related structure discussed below. Hence, any small change in the Drude properties of the ITO due to adsorption will have a significant effect on the $(\delta R/R)_p$ background in the mid-IR. Some variation (by as much as ~ 100 cm^{-1}) was noted in the energy of the plasmon resonance with sample preparation and with exposure to reagents. From the definition of ω_p given above, one finds $\delta n/n = 2(\delta\omega_p/\omega_p) = 2(\delta\omega_{min}/\omega_{min})$ for the relationship between small ($\ll 1$) fractional changes in n and ω_p. For a 40-nm-thick ITO film with $n = 7.0 \times 10^{20}$ cm^{-3} (i.e., an areal density of $n = 2.8 \times 10^{15}$ cm^{-2}), a $\delta(\hbar\omega_{min})$ of 50 cm^{-1} corresponds to an areal δn of 4.3×10^{13} cm^{-2}, that is, about 10% of an ML (see below). Hence, a change in the coverage of electrically active charge donors or acceptors by ~ 0.10 ML, as a result of sample treatment, could shift the plasmon resonance by 50 cm^{-1} (for an ITO film of $d = 40$ nm). Because of the limited availability of PLD ITO/Au samples, the effect of adsorption on the ITO Drude properties (also noted elsewhere[47,49]) has not been further investigated here. As a final comment, repeated application of the cleaning process described above (as many as seven cycles on one PLD sample) showed no significant loss of intensity in the plasmon resonance that would indicate erosion of the ITO film. For samples in which the Au/silica substrate had been properly cleaned prior to PLD growth, there was also no indication of delamination of the ITO film.

The origin of the weak shoulder at ~ 3950 cm^{-1} in Figure 1 (inset) is uncertain. A theoretical study[52] of defects in In_2O_3 has found that two types of interstitial In sites can form. These are labeled In_{i_a} and In_{i_c} and have ground states at 572 meV (4613 cm^{-1}) and 187 meV (1508 cm^{-1}), respectively, below the conduction band minimum. There is also an In vacancy (V_{In_d}) acceptor-type defect with an empty level in the ground state at 363 meV (2928 cm^{-1}) above the valence band maximum. These are the only defects with excitation energies predicted to lie within range of the present IR experiment. The ionization of an In_{i_a} donor would be reasonably close in energy to the ITO band in question, especially in the presence of a finite electron−hole interaction, which would reduce the energy of the optical transition relative to the theoretical ground-state ionization energy. Further investigation of this issue is beyond the scope of the present work.

The absence of any strong absorption bands in the mid-IR (500−4000 cm^{-1}) is consistent with previous results[48,53] for sputter-deposited ITO films. In a highly conducting metal oxide,[54] the free carriers screen the coupling between lattice modes and the external electromagnetic field. The IR-active lattice modes[55] of In_2O_3 powder fall below about 600 cm^{-1} and, due to imperfect screening in ITO, may give rise to the absorption evident in Figure 1 below ~ 600 cm^{-1}. It is significant that there is no indication of any feature in the 3200−3700 cm^{-1} region attributable to OH groups, either in the bulk or on the surface of the ITO. Numerical differentiation of the data in Figure 1, to suppress the strong, broad plasmon background in the O−H stretching region, did not reveal any relevant structure above the noise level.

For ITO dosed in situ with H_2O after Ar-ion bombardment in UHV, a narrow band is observed[2] at 3644 cm^{-1} due to isolated

(52) Tomita, T.; Yamashita, K.; Hayafuji, Y.; Adachi, H. *Appl. Phys. Lett.* **2005**, *87*, 051911.
(53) Wu, W.-F.; Chiou, B.-S. *Appl. Surf. Sci.* **1993**, *68*, 497.
(54) Cox, P. A.; Egdell, R. G.; Flavell, W. R.; Kemp, J. P.; Potter, F. H.; Rastomjee, C. S. *J. Electron Spectrosc. Relat. Phenom.* **1990**, *54/55*, 1173.
(55) White, W. B.; Keramidas, V. G. *Spectrochim. Acta* **1972**, *28A*, 501.

OH groups (i.e., those not hydrogen-bonded either to each other or to physisorbed H_2O). The surface preparation in this case produces a high OH coverage, due to reaction of the damaged surface with H_2O, and the small width of the isolated-OH absorption band increases its detectability. For a sample exposed to room air, physisorption of molecular H_2O would produce an O−H stretching band that is very broad and shifted to lower energy.[56] One previous study[12] used IR attenuated total reflection (ATR) spectroscopy to increase the sensitivity to surface species. In this case, ITO was sputter-deposited onto a Si ATR optical element and chemically cleaned. Reaction with an ethoxysilane species leads to the removal of a very broad O−H stretching band, which might be associated with physisorbed H_2O as well as with H-bonded surface OH groups. The present inability to detect the O−H stretching mode on chemically cleaned, air-exposed ITO concurs with previous high-resolution electron energy loss results[37] obtained for similar samples after mounting in UHV. Thus, it remains unclear whether surface OH sites (as distinct from physisorbed H_2O) can be detected in the O−H stretching region for chemically cleaned ITO exposed to room air.

3.2. Compositional Analysis of the ITO. The issues of the composition of commercial versus PLD ITO and of the effects of surface cleaning will now be considered. Several groups[36,37,57−66] have analyzed (mainly using XPS) the effects of various cleaning procedures on the composition of ITO surfaces, and others[67−69] have analyzed the bulk composition of ITO films. Cleaning by O_2 plasma and by UV/ozone treatment are the two most widely used approaches to reducing the surface C coverage. The former method has been most extensively characterized in refs 37, 58, 61, and 64 and the latter in refs 60 and 66.

It is appropriate at this point to note that several recent studies[70−75] have provided evidence for a stable chemisorbed oxygen entity, believed to be a peroxide (O_2^{2-}) species, on ITO surfaces cleaned by either an O_2 plasma or a UV/ozone treatment. This conclusion is based in part on ultraviolet photoemission spectroscopy (UPS) data, which are more surface-sensitive and chemically specific than core-level XPS data. One consequence of this oxygen enrichment is a passivation of donors at the ITO surface (termed a "chemical depletion" of free carriers[74]), which leads to an increase in the ITO work function. It is not known, however, if this adsorbed oxygen species survives the boiling-H_2O immersion used in the present work as the final step in surface preparation, and none of the results obtained here appear directly related to such an oxygen enrichment.

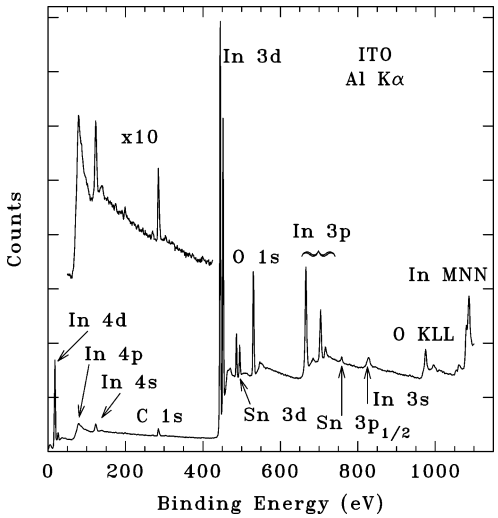

Figure 2. XPS survey data for PLD ITO film after cleaning by UV/ozone treatment followed by immersion in boiling H_2O, recorded at a photoelectron takeoff angle of $\theta = 0$ with respect to the surface normal. Various core-level and Auger features are labeled. Note that the Sn $3p_{3/2}$ peak, at a binding energy of about 715 eV, overlaps the plasmon satellite of the In $3p_{1/2}$ peak. The inset shows the BE range from 50 to 425 eV with a 10-fold vertical expansion. Emission from common impurities (Si 2p, BE ≈ 102 eV; S 2p, BE ≈ 165 eV; Cl 2p, BE ≈ 200 eV; N 1s, BE ≈ 400 eV) would be detectable in this range.

Figure 2 shows a typical XPS survey scan, recorded at a photoelectron takeoff angle of $\theta = 0$ with respect to the surface normal, for PLD ITO cleaned only by UV/ozone treatment (followed by immersion in boiling H_2O). The only obvious impurity signal is the C 1s, and there is no indication of Si 2p (∼102 eV), N 1s (∼400 eV), or other extraneous features sometimes detected at trace levels for ITO films (e.g., ref 61). There is also no Au 4f emission in the 84−87 eV range from the Au layer underlying the ITO, although in some cases a very weak Au 4f signal could be observed due to pinholes in the ITO film. As in virtually all previous XPS work on ITO, the present study uses Al Kα excitation. In the following, this source will be implicitly assumed in any discussion of relative peak intensities.

Table 1 gives typical results for the elemental composition of commercial and PLD ITO films after the complete cleaning procedure (solvent pre-clean; UV/ozone; boiling H_2O) described above. The method used to extract these results from the XPS peak areas is described in the Supporting Information. The O concentration is derived from the total O 1s intensity; however, a small fraction of the O 1s intensity (∼10%, see below) could be due to organic contaminants. If the ITO is formally described as $x{\cdot}In_2O_3 + (1 - x){\cdot}SnO_2$, then the PLD Sn/In concentration ratio in Table 1 gives $x = 0.79$ near the surface (i.e., within the $\theta = 0$ sampling depth of ∼19 Å). This is close to the composition of the source material used in PLD ($x = 0.83$, see Supporting Information).

If both oxides were fully stoichiometric, then the resulting PLD O/In concentration ratio would be $[3x + 2(1 - x)]/2x = 1.76$ instead of the value of 1.39 given in Table 1 for PLD ITO. This indicates that the ITO is oxygen-deficient, which is a general property of the material and which is responsible for the high conductivity.[67] The O/In and O/Sn concentration ratios in Table 1 are similar to those reported elsewhere[60] for UV/ozone-cleaned

(56) Hoffmann, P.; Knözinger, E. *Surf. Sci.* **1987**, *188*, 181.
(57) Kim, J. S.; Ho, P. K. H.; Thomas, D. S.; Friend, R. H.; Cacialli, F.; Bao, G.-W.; Li, S. F. Y. *Chem. Phys. Lett.* **1999**, *315*, 307.
(58) Christou, V.; Etchells, M.; Renault, O.; Dobson, P. J.; Salata, O. V.; Beamson, G.; Egdell, R. G. *J. Appl. Phys.* **2000**, *88*, 5180.
(59) So, S. K.; Choi, W. K.; Cheng, C. H.; Leung, L. M.; Kwong, C. F. *Appl. Phys. A: Mater. Sci. Process.* **1999**, *68*, 447.
(60) Song, W.; So, S. K.; Wang, D.; Qiu, Y.; Cao, L. *Appl. Surf. Sci.* **2001**, *177*, 158. Song, W.; So, S. K.; Cao, L. *Appl. Phys. A: Mater. Sci. Process.* **2001**, *72*, 361.
(61) Liau, Y.-H.; Scherer, N. F.; Rhodes, K. *J. Phys. Chem. B* **2001**, *105*, 3282.
(62) Kim, J.-S.; Cacialli, F.; Friend, R. *Thin Solid Films* **2003**, *445*, 358.
(63) Wu, C. C.; Wu, C. I.; Sturm, J. C.; Kahn, A. *J. Appl. Phys.* **1997**, *70*, 1348.
(64) You, Z. Z.; Dong, J. Y. *Appl. Surf. Sci.*, in press.
(65) Archambeau, S.; Séguy, I.; Jolinat, P.; Farenc, J.; Destruel, P.; Nguyen, T. P.; Bock, H.; Grelet, E. *Appl. Surf. Sci.*, in press.
(66) Sugiyama, K.; Ishii, H.; Ouchi, Y.; Seki, K. *J. Appl. Phys.* **2000**, *87*, 295.
(67) Fan, J. C. C.; Goodenough, J. B. *J. Appl. Phys.* **1977**, *48*, 3524.
(68) Nelson, A. J.; Aharoni, H. *J. Vac. Sci. Technol., A* **1987**, *5*, 231.
(69) Ishida, T.; Kobayashi, H.; Nakato, Y. *J. Appl. Phys.* **1993**, *73*, 4344.
(70) Lee, K. H.; Jang, H. W.; Kim, K.-B.; Tak, Y.-H.; Lee, J.-L. *J. Appl. Phys.* **2004**, *95*, 586.
(71) Golovanov, V.; Mäki-Jaskari, M. A.; Rantala, T. T.; Korotcenkov, G.; Brinzari, V.; Cornet, A.; Morante, J. *Sens. Actuators, B* **2005**, *106*, 563.
(72) Gassenbauer, Y.; Klein, A. *Solid State Ionics* **2004**, *173*, 141.
(73) Gassenbauer, Y.; Klein, A. *J. Phys. Chem. B* **2006**, *110*, 4793.
(74) Harvey, S. P.; Mason, T. O.; Gassenbauer, Y.; Schafranek, R.; Klein, A. *J. Phys. D: Appl. Phys.* **2006**, *39*, 3959.
(75) Gassenbauer, Y.; Schafranek, R.; Klein, A.; Zafeiratos, S.; Hävecker, M.; Knop-Gericke, A.; Schlögl, R. *Phys. Rev. B* **2006**, *73*, 245312.

Table 1. XPS Atomic Concentrations for Commercial and PLD ITO Samples after Cleaning[a]

element	commercial	PLD
In	37.4	39.6
Sn	5.8	5.1
O[b]	56.8	55.3
C[c]	2.52×10^{14} cm^{-2}	3.84×10^{14} cm^{-2}
x·$In_2O_3 + (1 - x)$·SnO_2[d]	$x = 0.76$	$x = 0.79$
O/In[e]	1.52 (1.82)	1.39 (1.76)

[a] Surface preparation in both cases was via solvent pre-cleaning followed by UV/ozone treatment and immersion in boiling H_2O (see text). All concentrations are in atomic fractions except for C, which is given as a surface concentration (see text). The photoelectron takeoff angle in both cases was $\theta = 0$ relative to the surface normal. Some dependence of composition on θ was observed (see text). [b] The O value is derived from the total O 1s signal from all components (cf., Figure 3). [c] For an estimated ITO surface atom density of 4.885×10^{14} cm^{-2} (see Supporting Information), the C coverage is $\Theta_C \approx 0.52$ ML for the commercial sample and 0.79 ML for the PLD sample. The difference is not thought to be significant. [d] For an ITO composition of x·$In_2O_3 + (1 - x)$·SnO_2, the value of x is given. [e] The value given is the O/In atom ratio, and the number in parentheses is what the ratio would be for a completely stoichiometric mixture (i.e., no O vacancies) of In_2O_3 and SnO_2 with the composition specified by x.

ITO measured in a normal-emission (i.e., bulk-sensitive) geometry. The small difference in impurity C coverage (Θ_C) for the two samples is not thought to be significant because Θ_C varies over the range of about 0.5−0.8 ML from run to run. For an estimated In concentration of 4.92×10^{21} cm^{-3} (see Supporting Information), the Sn concentration in PLD ITO is 6.34×10^{20} cm^{-3}, which is close to the electron density of $n = 7.0 \times 10^{20}$ cm^{-3} estimated from the measured plasmon frequency (see above) with $m^* = 0.40m_e$.

Finally, the dependence of composition on photoelectron takeoff angle (i.e., on sampling depth) was considered. For commercial ITO samples, the Sn/In atom ratio was typically ∼20% greater for $\theta = 60°$ than for $\theta = 0$, whereas the Sn/O atom ratio was essentially constant. This is consistent with previous results[59,60,63] for ITO cleaned by UV/ozone or mild O_2 plasma treatment and suggests that the surface is somewhat enriched in SnO_2 versus the bulk. This enrichment is a property of the as-grown material and is not disturbed by these cleaning methods. For PLD ITO, the Sn/In atom ratio was <10% greater for $\theta = 60°$, indicating only a small degree of Sn enrichment at the surface.

3.3. Surface Preparation and Composition. Figures 3 and 4 show O 1s and C 1s XPS data for a PLD ITO sample that was cleaned by UV/ozone treatment but which had not first been pre-cleaned by the sequence of solvents described above. These results are typical of ITO prepared by similar means, and the interpretation of these data is important in the present work.

Three O 1s components are clearly detected with the possible indication of a fourth, very weak feature in the vicinity of 529 eV, which is evident as a structure above the noise level in the residual spectrum. However, this fitting error can be eliminated, without the introduction of another component, simply by allowing a small Lorentzian character in the O_1 line (see below). Some previous ITO studies using oxygen plasma or UV/ozone cleaning found no such fourth, low-BE component.[57,60] Another study[61] reported a peak at 530.0 eV (in addition to the main O_1 peak at 530.5 eV) that gained intensity when the contamination layer on the as-received sample was removed by oxygen plasma cleaning. This low-BE feature, which is of uncertain origin, could be eliminated by Ar-ion bombardment,[61] which suggests that it is surface-related. A similar feature has also been observed[76] for ITO after oxygen plasma treatment and assigned to a Sn−O•

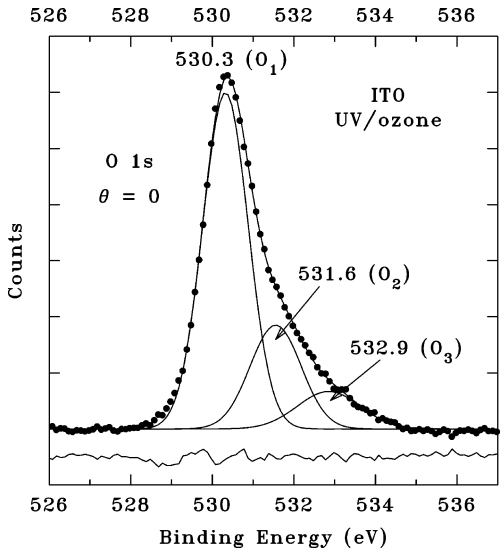

Figure 3. O 1s XPS data (corresponding to Figure 2) after least-squares fitting with a sum of three Gaussians and a quartic polynomial background function. The points show the raw data after subtraction of the fitted background. The peak energies of the three components are given (labeled as in Table 1), and the line through the points shows the sum of the three Gaussians. The residual (fit minus data, not statistically weighted) is also shown. The fwhm values are 1.31, 1.47, and 1.82 eV, respectively, for O_1, O_2, and O_3. The peak areas are in the ratio of 1.00:0.34:0.15 for O_1:O_2:O_3. The data were recorded at a photoelectron takeoff angle of $\theta = 0$ relative to the surface normal for a sample cleaned by UV/ozone treatment with no prior cleaning in organic solvents (see text).

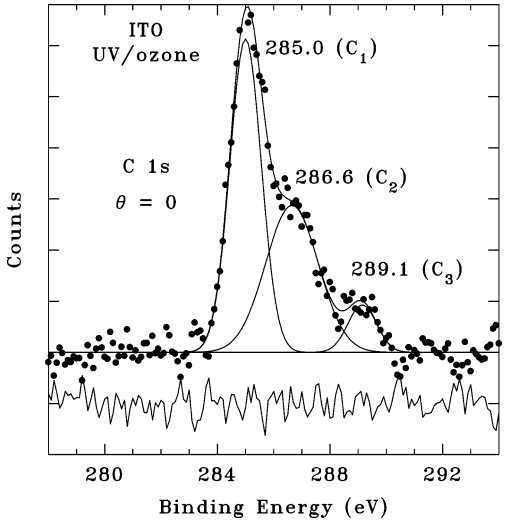

Figure 4. As in Figure 3 but showing C 1s data. The fwhm values are 1.31, 2.20, and 1.20, respectively, for C_1, C_2, and C_3, and the peak areas are in the ratio of 1.00:0.79:0.14.

surface radical. In subsequent O 1s fits, the main (O_1) peak will be allowed a variable degree of Lorentzian broadening (Γ_L), and the result returned by the fitting procedure is usually in the range of 0.12−0.16 eV, close to the value of $\Gamma_L \approx 0.15$ eV estimated from atomic spectroscopy data.[77]

The O_1-O_2 and O_2-O_3 peak separations of 1.3 eV are too large to be ascribed to free-electron plasmon excitation because the plasmon excitation energy, which corresponds to the maximum in $\mathrm{Im}(-1/\tilde{\epsilon})$ (see above), is $\hbar\omega_p/\sqrt{\epsilon_\infty} \approx 0.81$ eV. Hence, neither O_2 nor O_3 is thought to be a plasmon loss satellite,

(76) Milliron, D. J.; Hill, I. G.; Shen, C.; Kahn, A.; Schwartz, J. *J. Appl. Phys.* **2000**, *87*, 572.
(77) Krause, M. O.; Oliver, J. H. *J. Phys. Chem. Ref. Data* **1979**, *8*, 329.

Table 2. O 1s XPS Relative Peak Binding Energies (ΔBE)

assignment	this work (Figure 3)	reference 2	reference 36
bulk In_2O_3[a]	0.0 (O1, 530.3)	0.0 (530.5)	0.0 (529.6)
"sub-oxide"	1.3 (O2)	1.0	1.1
organic contam.		1.9	
OH ions[b]	2.6 (O3)	2.3	2.3
molecular H_2O	not obs.	3.8	~3.5

[a] The numbers in parentheses are the absolute O_1 BEs. The labels O_1, O_2, and O_3 refer to Figure 3. The O_1 BE in the present work is based on an impurity C 1s BE of 285.0 eV. Reference 2 reports a C 1s BE of 284.0 eV, but the O_1 BE has apparently been corrected appropriately. Reference 36 gives a C 1s BE of 284.9 eV, and the reported O_1 BE has been shifted 0.1 eV higher. [b] For air-exposed surfaces, other species are believed to contribute intensity at nearly the same ΔBE (see text).

as has been suggested to occur in In 3d XPS data.[58] No comparable features are observed in the present In 3d data (not shown). Such plasmon satellites are, however, observed[75] in O 1s and In 3d XPS data for highly reduced (i.e., O-deficient) ITO. Furthermore, the pronounced asymmetry to higher BE, evident in the raw O 1s data, cannot be attributed to the many-body effects commonly observed in the core-level XPS of free-electron metals (see, for example, ref 78) because no comparable asymmetry is observed in the In 3d spectrum (not shown).

The pattern of three O 1s peaks and their energy separations are in general agreement with previous work.[36,57,60,61] However, the relative intensities differ among the various studies, depending on the procedures for film growth and surface preparation. Obtaining unique least-squares fits of the O 1s data for ITO is particularly difficult (see below), and variations in the fine-structure found in different studies could also arise from differences in the fitting procedures. Such factors include the line shape assumed (pure Gaussian or Gaussian-broadened Lorentzian), the type of background function employed, and whether the background was subtracted before fitting or, as was done here, included in the fit. As a check on the correct identification of the O_1 peak in different studies, on which the computation of BE shifts (ΔBEs) depends, it was verified that the ΔBE between the O_1 and In $3d_{5/2}$ peaks is 85.6−85.7 eV in all cases. Thus, the different O 1s spectra have been correctly aligned, regardless of the absolute BEs, in comparing the results of different studies.

One ITO study,[2] combining IR and XPS measurements on surfaces in UHV (summarized in Table 2), provides a clear interpretation of the O 1s fine structure. Here, the main peak, due to stoichiometric In_2O_3, is seen at 530.5 eV, corresponding to O_1. A second peak (intermediate between O_2 and O_3) is seen at $\Delta BE = 1.9$ eV, which, together with the C 1s peak, is removed by in situ Ar-ion bombardment (see also ref 37). This feature is identified with O-containing organic contamination. Molecular H_2O, in the form of ice condensed on the ITO surface at 170 K, shows a peak at $\Delta BE = 3.8$ eV. No corresponding feature is evident in Figure 3. Formation of OH, by reaction of H_2O with the ion-bombarded surface,[2] gives a peak at $\Delta BE = 2.3$ eV. In addition, a peak is seen at $\Delta BE = 1.0$ eV for the ion-bombarded surface, corresponding to peak O_2 in Figure 3, which appears to lose some intensity upon subsequent H_2O exposure. The O_2 peak is ascribed to O-deficient "sub-oxide" sites associated with O vacancies, as proposed by others.[36,57] The O_2 peak has, in some studies, been assigned to O in SnO_2 versus In_2O_3. However, XPS data[71] for pure In_2O_3 also show a three-peaked structure, similar to that in Figure 3, with the main peak at a BE of 530.5 eV. For comparison, Table 2 also shows the results of a previous study[36] of chemically cleaned and air-exposed ITO.

The interpretation of peak O_3 as the signature of OH groups, on atomically clean surfaces prepared and maintained in UHV, appears to be conclusive in view of the results in ref 2. In this case, the O_3/O_1 relative intensity is about 0.2 for a surface with a maximal coverage of OH. The photoelectron takeoff angle, θ, was not reported in ref 2, but an increase in the intensity ratio by a factor of $\cos(0)/\cos(70°) = 2.9$ is expected in going from $\theta = 0$ to 70°. If every surface site had an adsorbed OH and if OH were the only contributor to the O_3 peak, an O_3/O_1 intensity ratio of ~0.3 would be estimated for $\theta = 0$ using the procedure given in the Supporting Information. Results for air-exposed surfaces[36,57,60,61] indicate a peak at about the same ΔBE with a large O_3/O_1 intensity ratio (exceeding unity, in some cases,[36] for $\theta = 75°$). According to the above estimate, assigning this peak exclusively to surface OH would require that nearly every surface cation site has an attached OH group. This high OH coverage is inconsistent with the results of titration experiments (see below) in which the ITO surface is exposed to reagents that react preferentially with OH groups. Angle-dependent XPS data[57,60] indicate that this intense O_3 peak is surface-related and thus cannot be ascribed to the introduction of a high density of OH into the bulk of the oxide.

It has been noted[36] that the relative intensity of the O_3 peak is uncorrelated with the reactivity of the ITO surface toward ferrocene, which reacts selectively with surface OH. It is, furthermore, recalled that practical ITO surfaces also exhibit a high coverage of C impurity, which might reduce the maximum attainable OH coverage. These results suggest that at least part of the O_3 peak intensity for air-exposed ITO derives from some species other than OH, such as an organic contaminant. The greater fwhm of O_3 (1.8 eV) versus O_1 (1.3 eV) further suggests the presence of unresolved, overlapping components. Additional information relating to the O_3 peak is given below.

Figure 4 shows C 1s data that provide information about the chemical state of the C impurity.[42] Although Ar^+-ion bombardment was not performed during the present study, others (e.g., refs 2 and 37) have noted that C is easily removed from ITO by such treatment, which indicates that the C is localized predominantly at the surface. Also, C 1s data (not shown) recorded under bulk- ($\theta = 0$) and surface-sensitive ($\theta = 60°$) conditions are virtually identical other than for a higher SNR in the former (due to a greater spectrometer efficiency). This contrasts with the O 1s data, which indicate chemically different surface and bulk species. Finally, the C 1s spectrum (Figure 2, inset), in contrast to the In, Sn, and O XPS features, shows only a weak (relative to the main peak) tail to higher BE. This tail, which is evident as a "step" between the low- and high-BE sides of the peak, arises from inelastically scattered photoelectrons, and its relative weakness in the C 1s spectrum is an indicator[79] of emission from atoms at or near the sample surface.

The C_1 peak, which is the BE calibration standard at 285.0 eV, is due to aliphatic C. The C_2 peak, at $\Delta BE = 1.6$ eV, could be due to C bonded to O in an alcohol (C−OH) or an ester (C−O−C), both of which are consistent with the O_3 satellite[42] in the O 1s spectrum (Figure 3). The larger fwhm of the C_2 peak (2.2 eV, vs 1.3 eV for C_1 and 1.2 eV for C_3) suggests contributions from more than one chemical species. The C_3 peak, at $\Delta BE =$ 4.1 eV, is in the range expected[42] for a carboxylic C atom (>C═O). Previous work[60] has indicated that C not removed by UV/ozone treatment remains on the ITO surface in a partially oxidized state, which is consistent with the observation that about one-half the total C 1s area in Figure 4 is contained in the C_2 and

(78) Citrin, P. H.; Wertheim, G. K.; Baer, Y. *Phys. Rev. B* **1977**, *16*, 4256.

(79) Tougaard, S. *Surf. Interface Anal.* **1998**, *26*, 249; *J. Vac. Sci. Technol., A* **1996**, *14*, 1415.

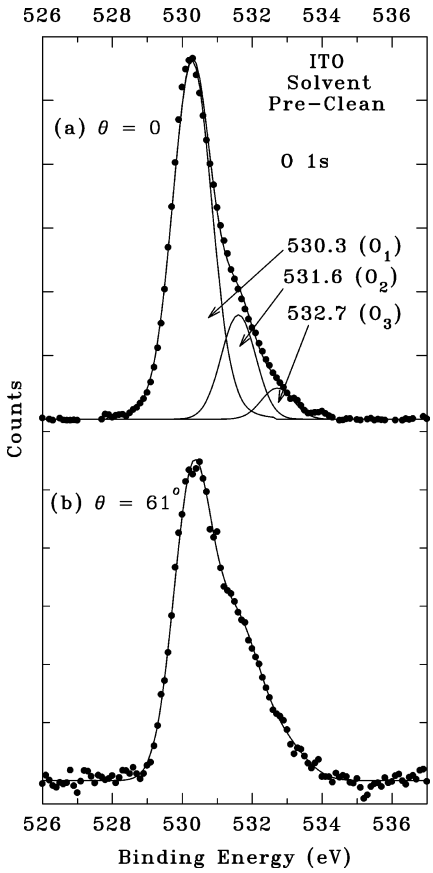

Figure 5. O 1s XPS data, as in Figure 3, but showing the effect of solvent pre-cleaning prior to UV/ozone treatment. The photoelectron takeoff angles are (a) 0 and (b) 61°, and the individual fitting components are shown only for the $\theta = 0$ data (see text). The peak areas in (a) are in the ratio of 1.00:0.25:0.069.

C_3 peaks. Given the estimate (Table 1) of $\Theta_C \approx 0.5-0.8$ ML, this implies the presence of roughly 0.2−0.4 ML of O in the form of various organic functional groups. This may be significant from the perspective of functionalization chemistry.

3.4. Solvent Pre-cleaning. We now consider the effect on surface composition of the solvent pre-cleaning procedure, described above, when performed prior to UV/ozone treatment. The effect of various organic solvents on ITO surface carbon contamination has been reported previously.[33] Figures 5 and 6 show XPS data corresponding to Figures 3 and 4, respectively, for samples subjected to solvent pre-cleaning and then to UV/ozone treatment. For simplicity, the fitting residuals are omitted from these and from subsequent data, but in all cases they are comparable to those in Figures 3 and 4 (UV/ozone only).

Figure 5a shows a somewhat smaller O_3/O_1 relative intensity than does Figure 3, which is evident even in the raw data as a slight narrowing of the high-BE edge of the peak. The data in Figures 3 and 5a were both recorded at $\theta = 0$. Given that the O_3 peak can be assigned, at least in part, to C−O−C and/or C−OH groups,[42] this is consistent with a lower concentration of oxidized C on the pre-cleaned surface. Figure 6 shows basically the same C 1s structure as does Figure 4 with the notable difference that the C_2/C_1 relative intensity is smaller by a factor of ∼2 for the solvent-treated sample, indicating a significantly lower coverage of C−O−C and/or C−OH groups. However, the C_3/C_1 relative intensity appears unaffected, which indicates that the concentration of >C═O species is unchanged. The difficulty in removing >C═O species is also evident in previous data.[33,65] In the following work, solvent pre-cleaning will be used to prepare

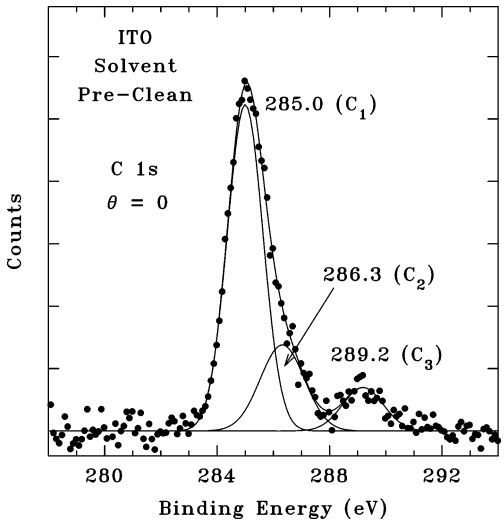

Figure 6. C 1s XPS data, as in Figure 4, but showing the effect of solvent pre-cleaning prior to UV/ozone treatment. The peak areas are in the ratio of 1.00:0.33:0.15.

surfaces for functionalization studies to reduce as much as possible the coverage of partially oxidized C sites.

One comment regarding the XPS line shape fitting is needed. The C 1s fits were "robust" in the sense that consistent and reproducible results were invariably obtained for different data sets. However, the O 1s fits were more difficult, especially under conditions of higher surface sensitivity (i.e., $\theta = 60°$) and/or for functionalized surfaces. This is attributed to the presence of multiple, unresolved components from different chemical species, the relative intensities of which vary with surface treatment and with θ. Attempts to fit such data lead to strong correlation[80] between different pairs of parameters, resulting in fits that are not unique and that are therefore unreliable regarding the intensity, position, and width of individual components. Consistent O 1s fits could be obtained only by introducing a constraint,[80] by fixing the energy of the main (O_1) peak at a position determined by inspection of the raw data. This procedure works reasonably well only at $\theta = 0$, for which O_1 is by far the dominant peak. Hence, Figure 5 shows O 1s data for $\theta = 0$ and 60°, but individual fitting components are given only for the former. For the latter, only the raw data (after subtraction of the fitted background) and the total fit are shown because no conclusions can be drawn from individual fitting components.

Measurements of the H_2O CA were used to document the rapid adsorption of contaminants when clean ITO surfaces are exposed to room air, because CA data can be recorded much more quickly than XPS data. Within 15 min after solvent pre-cleaning and UV/ozone treatment, but with no subsequent immersion in boiling H_2O, the CA was typically <10° but increased to between 10° and 20° after 1 h in ambient room air. An overnight exposure to room air increased the CA to ∼46°, beyond which little or no further change occurred. A similar aging effect on the CA has been noted elsewhere.[81] These results provide a qualitative indication of the rapid uptake of hydrophobic species (or the removal of hydrophilic sites). The small initial CA concurs with previous work[1] for UV/ozone-cleaned ITO; however, the initial CA reported after O_2 plasma cleaning[64,81] is higher, about 20−30°. In the present work, if the clean sample was instead placed in triply distilled H_2O for ∼1.5 h under ambient conditions, the CA increased to 17°; however, the chemical process occurring during H_2O immersion is unclear.

(80) Wertheim, G. K. *J. Electron Spectrosc. Relat. Phenom.* **1992**, *60*, 237.
(81) Zhong, Z. Y.; Jiang, Y. D. *Eur. Phys. J. Appl. Phys.* **2006**, *34*, 173.

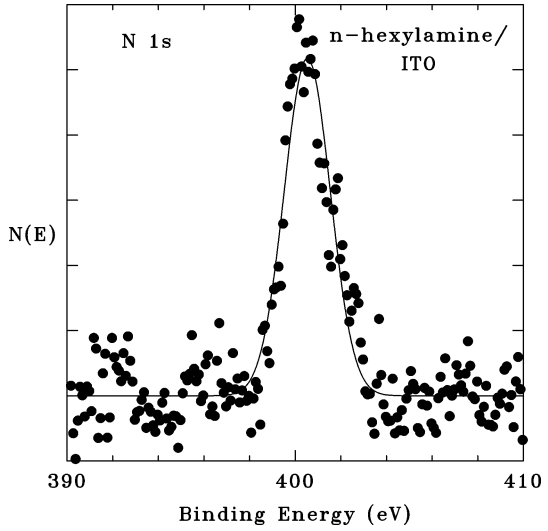

Figure 7. N 1s XPS data for ITO after a 5-h exposure to *n*-hexylamine vapor. The points show the raw data, after subtraction of the fitted polynomial background, and the line shows the fit with a single Gaussian.

3.5. Functionalization. *3.5.1. n-Hexane and n-Hexylamine.* The reaction with *n*-hexylamine was studied to assess the contribution, if any, from Lewis acid sites. Exposing an ITO sample to the vapor for 1 h resulted in a small coverage of adsorbed amine, estimated to be ∼0.08 ML based on the (N 1s)/(In $3d_{5/2}$) XPS intensity ratio using procedures described in the Supporting Information. An exposure of 5 h gave the same coverage, indicating that saturation is achieved for the 1-h treatment. Adsorbate coverages in MLs, given here and in the following sections, are obtained by dividing the measured coverage in molecules per cm^2 by 4.885×10^{14}, a representative value for the number of ITO surface sites per cm^2 (see Supporting Information). This is simply a normalizing factor that converts the coverage unit from species per cm^2 to a more convenient one of a fraction of an ML. The magnitude of the resulting ML value is believed to be quantitatively reliable, but, in any case, uncertainty in this normalization factor has no effect on relative coverages.

The N 1s emission consisted of a single peak (Figure 7) with a BE of 400.4 eV and a fwhm of ∼2.2 eV. Adsorption can occur either through a Lewis acid−base interaction, involving electron transfer from the N lone-pair orbital to an acceptor site, or through a Brønsted acid−base interaction involving proton transfer to the amine. One argument against the latter is that the saturation coverage of adsorbed amine (∼0.08 ML) is considerably less than the OH coverage on the ITO surface, which is estimated (see below) to be about 0.21 ML. Another observation is that the N 1s BE for an adsorbate[82] with a free $-NH_2$ group (i.e., one that is not bonded to the surface) is about 400.1 eV, based on a C 1s BE of 285.0 eV. Relative to this value, ΔBE for the N 1s level of *n*-hexylamine adsorbed on ITO is only +0.3 eV. For NH_3 adsorbed on aluminosilicates[83] (mordenites), ΔBE, relative to NH_3 physisorbed at low temperature on an oxide-free Si(001) surface,[84] is approximately 0, +1.4, and +3.3 eV for adsorption at Lewis, weak Brønsted (Si−OH), and strong Brønsted (Al−OH−Si bridge) acid sites, respectively. Large N 1s ΔBEs are also seen[85] for NH_3 adsorbed at Brønsted- and strong Lewis-acid sites on faujasite-type zeolites.

These observations suggest that adsorption in the present case involves a weak Lewis acid−base interaction. The identity of the active site is unknown at present. However, because Sn comprises about 16% of the total surface cation concentration on the commercial ITO samples (allowing for the small increase in surface vs bulk Sn/In ratio), it is tempting to speculate that Sn sites are involved. Charge donation from an amine would be an alternative to oxygen vacancy formation as a means of reducing the positive charge on an Sn^{4+} ion substituting for an In^{3+} ion in In_2O_3. A study of NH_3 adsorption on OH-free SnO_2 (110) surfaces,[86] using UPS and temperature-programmed desorption, found a weak interaction with five-coordinate Sn^{4+} surface sites but more strongly acidic behavior on the part of four-coordinate Sn^{2+} sites at O vacancies. However, relating these results to the present data is difficult because the electronic structure of Sn at the surface of air-exposed ITO is uncertain.

The C 1s and O 1s data (not shown) exhibited no significant differences in structure from those of the unexposed surface. The C 1s peak for a $-CH_2-NH_2$ group is known[42] to appear at ΔBE = 0.94 eV relative to the aliphatic (C_1) peak, but this feature was not resolved in the present data. From the (C 1s)/(N 1s) XPS intensity ratio, a C/N atom ratio of ∼11.4 was found, which is consistent with the total C coverage being the sum of contributions from pre-existing impurities and from the adsorbate. The molecular coverage of ∼0.08 ML means a coverage of ∼0.48 ML of C from the adsorbed *n*-hexylamine alone. If that simply adds to the ∼0.5 ML of C due to organic impurities on the starting ITO surface, the (total C)/N atom ratio would then be ∼12.2. The precision limit in the C/N atom ratios is estimated to be a few percent, based on the uncertainty in the peak area determinations. As noted above, beam damage is not entirely negligible, and a decrease in the C/N atom ratio by about 30% was noted during several hours of XPS data collection.

In one experiment, a clean ITO sample was exposed to pure *n*-hexane vapor for 1 h. The resulting C coverage was within the range typically found for clean surfaces, and the C 1s XPS was virtually identical to that of an unexposed sample. In view of the lack of any clear indication of adsorption of *n*-hexane, it is concluded that *n*-hexylamine adsorbs via the $-NH_2$ group and that adsorption of other reagents also involves the reactive functional group(s) rather than the alkyl chain.

Some CA data were obtained after a 1- or 5-h amine exposure, followed by XPS data collection and subsequent exposure to air. The CA value of about 48−52° was essentially the same as for samples handled similarly but with no amine exposure. This suggests that any effect of the amine on the CA is small (consistent with the low coverage) and masked by the effect of air exposure.

The IRRAS data for *n*-hexylamine on ITO will be discussed below in connection with results for OTMS.

3.5.2. n-Octyltrimethoxysilane. A 1-h exposure to OTMS vapor led to an adsorbate coverage of about 0.16 ML, based on the (Si 2p)/(In $3d_{5/2}$) XPS intensity ratio. A 5-h exposure gave a somewhat higher value, ∼0.21 ML, which is assumed to represent the saturation coverage. The saturation coverage of OTMS is about 2.5 times higher than that of *n*-hexylamine, which could indicate that surface OH sites are more prevalent than Lewis acid sites or that OTMS is more effective at displacing hydrocarbon impurities (see below). A weak N 1s peak was detected after OTMS exposure, presumably due to an impurity in the reagent

(82) Moon, J. H.; Kim, J. H.; Kim, K.; Kang, T.-H.; Kim, B.; Kim, C.-H.; Hahn, J. H.; Park, J. W. *Langmuir* **1997**, *13*, 4305.
(83) Remy, M. J.; Genet, M. J.; Lardinois, P. F.; Notté, P. P.; Poncelet, G. *Surf. Interface Anal.* **1994**, *21*, 643.
(84) Dufour, G.; Rochet, F.; Roulet, H.; Sirotti, F. *Surf. Sci.* **1994**, *304*, 33.
(85) Guimon, C.; Zouiten, A.; Boreave, A.; Pfister-Guillouzo, G.; Schulz, P.; Fitoussi, F.; Quet, C. *J. Chem. Soc., Faraday Trans.* **1994**, *90*, 3461.
(86) Abee, M. W.; Cox, D. F. *Surf. Sci.* **2002**, *520*, 65.

vapor. The N coverage was about 0.028 (0.048) ML after a 1 (5)-h OTMS treatment, but there was no obvious correlation between the N coverage and other features in the XPS data.

The CA after a 1-h exposure to OTMS vapor was 87°, indicating a hydrophobic surface consistent with an adsorbed alkyl layer. A 5-h exposure resulted in a ∼20% larger CA of 104°, which is consistent with the ∼30% higher coverage. For comparison, another study[9] of ITO after treatment with OTMS found a CA of 95°. In this case, the ITO was cleaned using organic solvents, followed by treatment with an H_2O_2:NH_4OH:H_2O solution, and the functionalization reaction employed a solution of OTMS in dry toluene.

Assuming that OTMS adsorbs by reaction with surface OH groups, the saturation coverage of ∼0.21 ML reflects the coverage of such species. Previous work has used the reaction with organometallic reagents to titrate OH groups on ITO surfaces. For samples prepared by detergent cleaning followed by treatment with organic solvents,[6,36] a coverage of $(3-4) \times 10^{13}$ OH cm^{-2} was found (0.06−0.08 ML according to the definition of an ML given above). Subsequent exposure to an air plasma yielded $\sim 1.08 \times 10^{14}$ OH cm^{-2} (∼0.22 ML), the highest value for any surface preparation method reported in ref 36. Hence, the current estimate of the OTMS saturation coverage is consistent with what is known, on the basis of titration measurements, about the OH coverage on ITO surfaces, assuming that OTMS and the reagents used in refs 6 and 36 all react quantitatively and with one adsorbate per OH group (see below). It is also noted that the OH coverage found here for ITO is significantly less than for a fully hydroxylated SiO_2 surface, which is estimated[87] to be 5×10^{14} OH cm^{-2}. The results given thus far are for commercial ITO samples. The PLD samples, exposed to OTMS vapor as part of the IRRAS experiments discussed below, gave similar results except that the saturation coverage was lower, about 0.11 ML.

The present estimate of OH coverage (on the commercial ITO samples) implies an average distance of about 10 Å between nearest-neighbor sites, assuming a square-planar array, which is too large for an −O−Si−O− bridge. This supports the assumption that only one Si−O−M (M = In or Sn) bond forms per adsorbed OTMS. In principle, cross-linking between nearest-neighbor OTMS sites could occur via an H_2O elimination reaction between Si−OH sites formed by hydrolysis in room air of unreacted Si−OCH_3 groups. The structure formed would be essentially M−O−Si−O−Si−O−M (M = In or Sn). For In−O and Si−O bond lengths of 2.17 and 1.84 Å, respectively (based on the atomic covalent radii), a ∼120° −O−Si−O− bond angle and a ∼45° angle between the In−O bond and the surface plane (based on the In_2O_3 crystal structure given in the Supporting Information), a distance of about 9.44 Å between adsorption sites would be required for cross-linking to occur without bond strain. In the case of PLD ITO, the OH coverage is smaller by a factor of 2, resulting in an average distance of about 14 Å between adsorption sites, which effectively rules out the possibility of cross-linking.

The C/Si atom ratio, derived from the (C 1s)/(Si 2p) XPS intensity ratio, was about 7.3 before prolonged X-ray exposure. An OTMS saturation coverage of 0.21 ML means $8 \times 0.21 =$ 1.68 ML of C from the OTMS alone. If the adsorbate C adds to the ∼0.5 ML of impurity C on the initial ITO surface, the (total C)/Si atom ratio would be about 10.4. The measured values are somewhat smaller than the ideal (undamaged OTMS only) value of 8.0, suggesting that impurity species are displaced by the OTMS but also that beam damage is a factor. Previous studies of alkoxysilane adsorption on hydroxylated Si(100) surfaces[88] have also observed a displacement of preadsorbed impurities in IR-spectroscopic data.

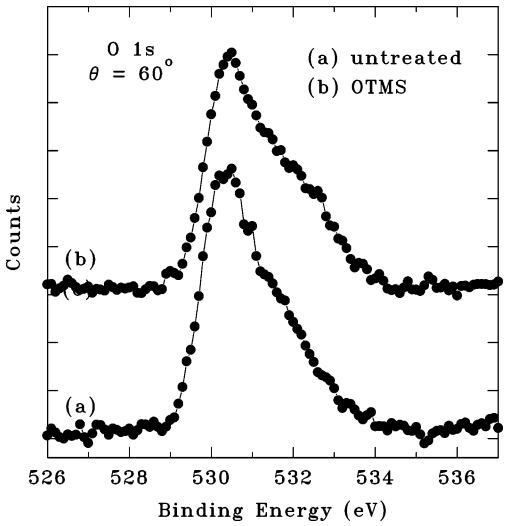

Figure 8. Raw (unfitted) surface-sensitive O 1s data ($\theta = 60°$) for ITO before and after exposure to OTMS. The spectra have been shifted vertically for clarity and have been scaled so as to give approximately the same maximum intensity.

Figure 8 shows the raw, surface-sensitive O 1s data ($\theta = 60°$, not fitted) for an unexposed surface and for a 5-h exposure to OTMS vapor. The latter is essentially the same as for a 1-h exposure. The main point to note is the small increase in the relative intensity of the high-BE shoulder, which is evident in the raw data even without fitting. This is consistent with the formation of Si−OH by hydrolysis in room air of unreacted Si−OCH_3 groups. For an OTMS molecule reacting with OH on the ITO surface, two OH groups are formed by hydrolysis for every OH removed by adsorption. Figure 9 shows surface- and bulk-sensitive C 1s XPS data for a 1-h exposure, which are again essentially the same as for a 5-h treatment. The data are similar to that of the unexposed surface (Figure 6) but with a much greater relative intensity in the alkyl (C_1) peak. This indicates that almost all C is in the alkyl sp^3-bonded form. Because all C is on the surface (i.e., there is no bulk C), the C 1s spectrum is independent of θ other than for a higher SNR at $\theta = 0$.

The Si 2p spectrum (Figure 10) can be fitted with a single spin−orbit doublet at a BE of 102.5 eV, in agreement with the BE of 102.67 ± 0.1 eV reported[89] for a siloxane of the form $CH_3Si(-O-)_3$. In performing the fit, the $2p_{1/2}-2p_{3/2}$ splitting and branching ratio were fixed at 0.602 eV and 0.53, respectively, as in elemental Si,[90] because these quantities are essentially independent of the chemical environment. A previous study,[91] reporting XPS data for metal oxides exposed to $H_2N-(CH_2)_3-Si(OC_2H_5)_3$, found evidence for a decomposition reaction leading to insertion of Si into the lattice. In the present work, an ITO functionalization experiment was performed using $H_2N-(CH_2)_3-Si(CH_3)_2(OC_2H_5)$, and two Si 2p peaks were found. One, at a BE of 101.9 eV, corresponds to that seen[89] (at a BE of 101.63 ± 0.1 eV) for a siloxane of the form $(CH_3)_3Si(-O-)$. It is not possible to determine, from the Si 2p BE alone, whether adsorption

(87) Zhuravlev, L. T. *Langmuir* **1987**, *3*, 316.

(88) Harder, P.; Bierbaum, K.; Woell, Ch.; Grunze, M.; Held, S.; Effenberger, F. *Langmuir* **1997**, *13*, 445.

(89) O'Hare, L.-A.; Parbhoo, B.; Leadley, S. R. *Surf. Interface Anal.* **2004**, *36*, 1427.

(90) Wertheim, G. K.; Riffe, D. M.; Rowe, J. E.; Citrin, P. H. *Phys. Rev. Lett.* **1991**, *67*, 120.

(91) Moses, P. R.; Wier, L. M.; Lennox, J. C.; Finklea, H. O.; Lenhard, J. R.; Murray, R. W. *Anal. Chem.* **1978**, *50*, 576.

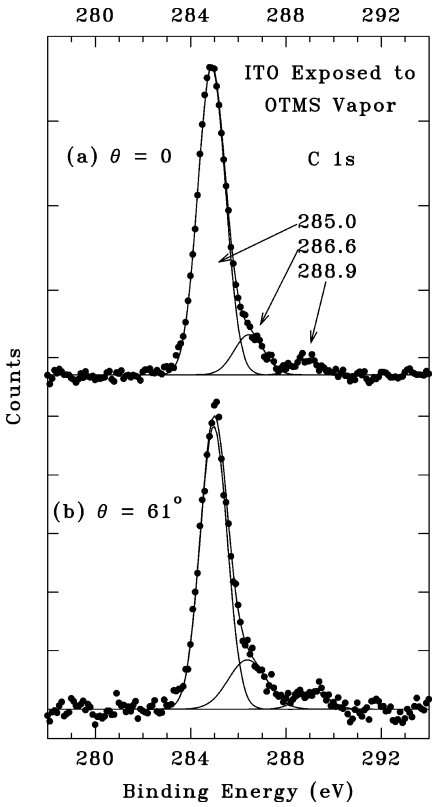

Figure 9. C 1s data as in Figure 6 but showing data recorded at photoelectron takeoff angles of (a) 0 and (b) 61° after exposure OTMS vapor. The fitted peak positions are indicated. The relative intensity of the two data sets is not to scale. The areas in (a) are in the ratio 1.00:0.14:0.049.

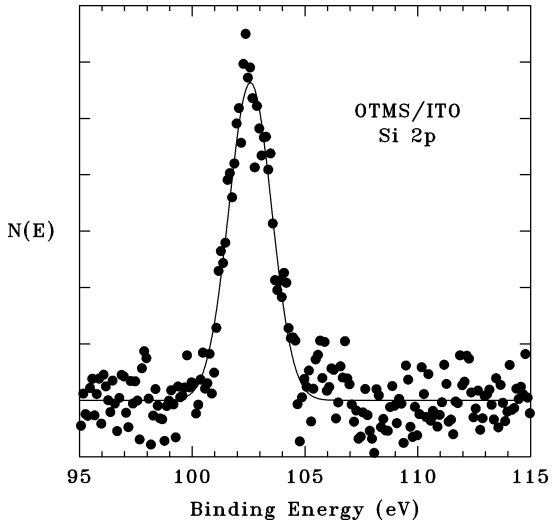

Figure 10. Si 2p XPS data for ITO after a 5-h exposure to OTMS vapor. The points are the raw data, after subtraction of the fitted polynomial background, and the line shows the fit with a single Gaussian spin−orbit doublet.

occurs via the amine or the siloxane group because either process would result in an adsorbate with a single Si−O bond. The other Si 2p peak, with a ∼10% smaller integrated intensity and a BE of 103.6 eV, is consistent[89] with Si 4-fold coordinated to O, which can form only by insertion of Si into the oxide lattice. However, the absence of a similar feature for OTMS argues against the occurrence in this case of a Si insertion process, which may be characteristic of alkoxysilanes with a short alkyl chain and/or an $-NH_2$ termination.

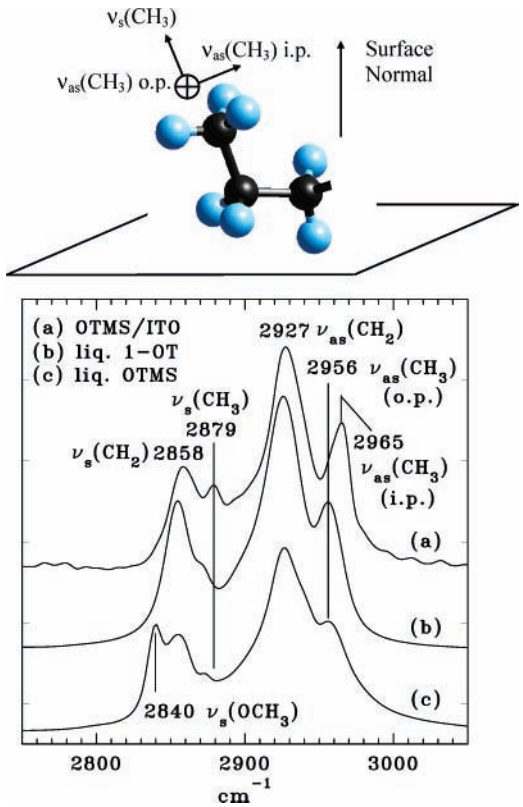

Figure 11. IRRAS data showing the C−H stretching region for (a) OTMS adsorbed on ITO, (b) liquid 1-octanethiol, and (c) liquid OTMS. The diagram shows a schematic model for the terminal $-CH_3$ group of the alkyl chain with the $CH_3-CH_2-CH_2-$ plane oriented normal to the surface. The approximate orientations of the $-CH_3$ dynamic dipole moments are indicated, and "i.p." and "o.p." refer to "in-plane" and "out-of-plane", respectively. The $\nu_s(CH_3)$ and $\nu_{as}(CH_3)$(i.p.) modes are polarized in the $CH_3-CH_2-CH_2-$ plane, while the $\nu_{as}(CH_3)$(o.p.) mode is polarized perpendicular to the plane. All spectra are plotted on an absorbance scale, with each spectrum scaled arbitrarily for approximately the same intensity at the 2927 cm^{-1} $\nu_{as}(CH_2)$ peak and shifted vertically for clarity.

Figure 11 compares IRRAS data in the C−H stretching region for OTMS on ITO with those for the randomly oriented *n*-octyl chain in liquid 1-octanethiol [$CH_3-(CH_2)_6-CH_2SH$, 1-OT] and for liquid OTMS. The spectrum of adsorbed OTMS was referenced to that of the bare ITO sample, and a polynomial background was subtracted. The liquid data were obtained by transmission through thin films captured between two salt plates and referenced to spectra of the bare plates. The 1-OT spectrum is typical for a randomly oriented 1-alkyl chain,[92] and the various mode assignments and polarization properties indicated in Figure 11 have been discussed at length elsewhere.[93] For comparison, a 15-h OTMS exposure (not shown) was done on a fresh sample because an extended treatment might enhance the formation of an ordered adsorbate layer. The same structure, relative intensities, and peak energies were found but with less intensity to either side of the $\nu_{as}(CH_2)$ mode, which might indicate a somewhat higher degree of ordering (see below).

The first point to note is that the relative intensity of the $\nu_s(CH_2)$ and $\nu_{as}(CH_2)$ modes is similar for adsorbed OTMS and liquid 1-OT. This indicates that the $-CH_2-$ chain in the former is essentially disordered, with no preferred stereoisomer. For example, in the all-trans configuration found in *n*-alkylthiol SAMs

(92) Porter, M. D.; Bright, T. B.; Allara, D. L.; Chidsey, C. E. D. *J. Am. Chem. Soc.* **1987**, *109*, 3559.
(93) Parikh, A. N.; Allara, D. L. *J. Chem. Phys.* **1992**, *96*, 927.

and in related molecular crystals, the dynamic dipole moments (DDMs) of $\nu_s(CH_2)$ and $\nu_{as}(CH_2)$ are oriented parallel and perpendicular, respectively, to the plane defined by the C backbone. Recalling the metal surface selection rule mentioned above, one finds that placing such a chain in any specific orientation with respect to the surface normal will then lead to a difference in relative intensity from that of a randomly oriented chain (see, for example, ref 93). Another indication of disorder in the alkyl chain is the energy of the $\nu_{as}(CH_2)$ mode, which depends on both chain length and order.[92] For a SAM formed by 1-OT adsorbed on Au in an all-trans configuration, this mode occurs at 2921 cm^{-1}, which is significantly lower than that for either liquid 1-OT (2926 cm^{-1}) or adsorbed OTMS (2927 cm^{-1}).

The situation discussed above changes when the $-CH_3$ modes are examined. The out-of-plane $\nu_{as}(CH_3)$(o.p.) mode, which is strong relative to the in-plane $\nu_{as}(CH_3)$(i.p.) mode in liquid 1-OT (ref 92), is absent (or at least strongly attenuated) in adsorbed OTMS, and the normally weaker $\nu_{as}(CH_3)$(i.p.) and $\nu_s(CH_3)$ modes are clearly observed. As diagrammed in Figure 11, the $\nu_s(CH_3)$ DDM lies parallel to the CH_3–C bond, the $\nu_{as}(CH_3)$(i.p.) DDM lies perpendicular to the CH_3–C bond but parallel to the $CH_3-CH_2-CH_2-$ plane, and the $\nu_{as}(CH_3)$(o.p.) DDM is normal to the CCC plane.

The differences in the CH_3 modes between adsorbed OTMS and liquid 1-OT can then be explained if the terminal CCC plane in OTMS is essentially perpendicular to the ITO surface, that is, if the CH_3-C bond projects upward from the surface as shown in Figure 11. In this configuration, the DDMs of $\nu_s(CH_3)$ and $\nu_{as}(CH_3)$(i.p.) have finite projections on the surface normal, but the $\nu_{as}(CH_3)$(o.p.) DDM does not. It should be noted that the DDMs are defined with respect to the CCC plane and do not change with rotation about the CH_3–C bond. However, the alkyl chain would have to lie essentially flat on the surface to inhibit rotation about the CH_3CH_2–C bond, which would "scramble" the polarization properties discussed here.

Figure 11 also shows that the CH_3O- modes of liquid OTMS are absent in adsorbed OTMS, indicating that essentially all such groups have reacted either with the surface or with H_2O in room air. In liquid CH_3OH, $\nu_s(CH_3)$ and $\nu_{as}(CH_3)$ appear at 2834 and 2947 cm^{-1}, respectively.[94] In liquid OTMS, the former is seen clearly at 2840 cm^{-1}, while the latter falls between the $\nu_{as}(CH_3)$-(o.p.) mode (at 2956 cm^{-1}) and the $\nu_{as}(CH_2)$ mode (at 2927 cm^{-1}) where it fills in the gap between them. There is no obvious orientation of the CH_3O- groups that would cause both modes to disappear from the spectrum of adsorbed OTMS if such groups were present.

Figure 12 compares IRRAS data for *n*-hexylamine and OTMS, both adsorbed on ITO. The smaller overall intensity of the amine spectrum reflects the lower saturation coverage versus OTMS. In Figure 12b, the $-CH_3$ modes are less well-defined than for OTMS, indicating a lesser degree of ordering of the terminal $-CH_3$ group. In particular, the $\nu_{as}(CH_3)$ peak appears to be broadened to lower energy, which suggests that the $\nu_{as}(CH_3)$-(i.p.) and (o.p.) modes are both contributing intensity.

4. Summary

The preparation and functionalization of ITO surfaces have been studied using primarily XPS and IRRAS and the reagents *n*-hexylamine and OTMS. Particular attention has been paid to the chemical characterization of the surfaces both before and after functionalization. The results are as follows.

(1) Surfaces cleaned by UV/ozone treatment and subsequently exposed to room air typically have about 0.5−0.8 ML of adsorbed impurity carbon. Most is in the form of aliphatic species, but as much as one-half the total C is partially oxidized and consists of C−OH, C−O−C, and/or >C═O groups. A substantial fraction of the O-containing C species results from oxidation of C on the initial surface by the UV/ ozone exposure, and the coverage of C−OH and/or C−O−C species (but not of >C═O groups) can be reduced by cleaning in a series of organic solvents prior to UV/ozone treatment.

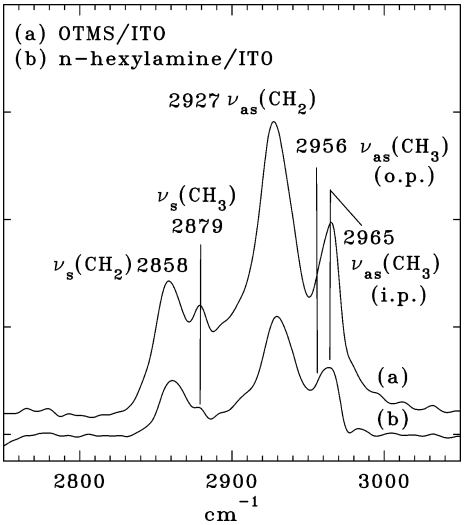

Figure 12. Similar to Figure 11 but showing data for (a) OTMS and (b) *n*-hexylamine adsorbed on ITO. Spectrum (a) is identical to that in Figure 11a. The peak labeling is the same as in Figure 11, and the spectra have been displaced for clarity. The relative intensity of the two spectra is approximately quantitative. The spectra are plotted on an absorbance (A) scale, where $A = -\log(R_p^{exp}/R_p^{bare}) = -\log_e[1 + (\delta R/R)_p]/2.303 \approx -(\delta R/R)_p/2.303$, and the tick marks are spaced at intervals of 2×10^{-4} absorbance units.

(2) The OH coverage on the ITO surfaces studied here is relatively small ($\sim$0.21 ML = 1.0×10^{14} OH cm^{-2} = 1.0 OH nm^{-2}), based on the Si coverage after reaction with alkoxysilanes. A satellite feature in the O 1s XPS spectrum, often suggested to be a quantitative measure of adsorbed OH, receives a significant contribution from O in organic contaminants and possibly from other sources not directly related to hydroxylated ITO. A better gauge of OH coverage is by titration with reagents that react with surface OH, followed by XPS analysis to determine adsorbate coverage. The present OH coverage estimate agrees quantitatively with other such determinations based on titration.

(3) The present work is, to our knowledge, the first side-by-side comparison of the surface composition and chemical properties of commercial and PLD ITO samples. The two materials appear to be essentially the same in this regard, but the OH coverage on the PLD material appears to be lower by a factor of about 2.

(4) *n*-Hexylamine adsorbs, at a saturation coverage of about 0.08 ML, via a weak Lewis acid−base interaction. The particular acid site has not been conclusively identified, but it is speculated that surface Sn sites may be involved. Adsorption of the amine does not appear to displace a significant fraction of the preadsorbed organic impurities from the ITO surface.

(5) For OTMS, the C/Si atom ratios suggest that some displacement of preadsorbed organic impurities from the ITO surface occurs during adsorption. This derives from the observation that the (total C)/Si ratio is always significantly less than would be expected if the C associated with OTMS simply added to the impurity C. However, molecular decomposition stimulated by X-ray radiation and/or by secondary electrons, while relatively

(94) Bertie, J. E.; Lan, Z. *J. Chem. Phys.* **1996**, *105*, 8502.

slow under the present experimental conditions, makes a quantitative determination difficult.

(6) For OTMS adsorbed on ITO, the alkyl chain is disordered, with no preferred stereoisomer. However, the chain appears to lie mainly parallel to the surface with the plane defined by the terminal $CH_3-CH_2-CH_2-$ segment oriented essentially perpendicular to the surface, as shown by the IR polarization properties of the C−H stretching modes of the $-CH_3$ group. Adsorbed *n*-hexylamine exhibits a lesser degree of ordering of the terminal $CH_3-CH_2-CH_2-$ segment.

Forming a well-ordered organic SAM on ITO, via a chemical process involving surface OH groups, may require a higher adsorbate packing density (and, therefore, a higher initial OH coverage) than can be achieved using the surface preparation methods described here. Damaging the ITO surface by Ar^+ bombardment, followed by in-situ exposure to H_2O vapor[2] or by ex-situ exposure to room air,[1] is a viable method for increasing the coverage of reactive surface OH sites.

(7) The free-electron plasmon resonance, easily detected in a BML IRRAS experiment, is sensitive to surface-chemical effects. These include sample-dependent shifts in energy as a result of repeated cleaning cycles and of exposure to reagents.

One important issue, not addressed here or, to our knowledge, in previous work, has to do with the effect of the SnO_2 additive on the ITO surface properties. To this end, a comparison of pure In_2O_3 with ITO would be most valuable. Another outstanding question relates to the functionalization properties of an atomically clean and undamaged ITO surface, as opposed to one that is either contaminated or else clean but damaged by ion bombardment. Recently, significant progress in this direction has been made by Gassenbauer at al., who have prepared and characterized ITO surfaces in situ under UHV conditions.[72−75] Finally, the effects of sample treatment on the plasmon resonance, noted in passing here, could provide information about the correlation between surface chemical and electronic properties of ITO. These sorts of IRRAS experiments would benefit greatly from parallel measurements of electrical conductivity[95] to separate the effects of changes in carrier density and scattering lifetime.

Acknowledgment. V.M.B. and A.D.B. contributed equally to this work. This work was supported by the Office of Naval Research. We thank R. E. Mowery for the use of his InSb detector in one of the IR experiments and D. Y. Petrovykh and N. Turner for helpful discussions on surface analysis. We are grateful to J. P. Long for discussions leading to the inception of this work.

Supporting Information Available: NMR and IR spectra of reagents; conditions for ITO thin-film growth by PLD; procedure for quantifying XPS peak intensities; IRRAS of adsorbates on ITO in a BML configuration. This material is available free of charge via the Internet at http://pubs.acs.org.

LA061578A

(95) Tobin, R. G. *Surf. Sci.* **2002**, *502−503*, 374.